Accepted Manuscript

Azaindole-BODIPYs: Synthesis, fluorescent recognition of hydrogen sulfate anion and biological evaluation

Gürkan Keşan, Burcu Topaloğlu, Emrah Özcan, Hasan Hüseyin Kazan, Esra Tanrıverdi Eçik, Elif Şenkuytu, Ibrahim F. Sengul, Hakan Kandemir, Bünyemin Çoşut

PII:	S1386-1425(19)30056-3
DOI:	https://doi.org/10.1016/j.saa.2019.01.047
Reference:	SAA 16733
To appear in:	*Spectrochimica Acta Part A: Molecular and Biomolecular Spectroscopy*
Received date:	17 July 2018
Revised date:	7 December 2018
Accepted date:	15 January 2019

Please cite this article as: Gürkan Keşan, Burcu Topaloğlu, Emrah Özcan, Hasan Hüseyin Kazan, Esra Tanrıverdi Eçik, Elif Şenkuytu, Ibrahim F. Sengul, Hakan Kandemir, Bünyemin Çoşut , Azaindole-BODIPYs: Synthesis, fluorescent recognition of hydrogen sulfate anion and biological evaluation. Saa (2019), https://doi.org/10.1016/j.saa.2019.01.047

Azaindole-BODIPYs: Synthesis, Fluorescent Recognition of Hydrogen Sulfate Anion and Biological Evaluation

Gürkan Keşan[a], Burcu Topaloğlu[a], Emrah Özcan[a], Hasan Hüseyin Kazan[b], Esra Tanrıverdi Eçik[a], Elif Şenkuytu[a], Ibrahim F. Sengul[a], Hakan Kandemir[c], Bünyemin Çoşut[a*]

Contribution from:

[a] Department of Chemistry, Faculty of Science, Gebze Technical University, Gebze, Kocaeli, Turkey

[b] Department of Biological Sciences, Middle East Technical University, Ankara, Turkey

[c]Department of Chemistry, Faculty of Art and Science, Namık Kemal University, Tekirdag, Turkey

[*]Author for correspondence:

Dr. Bünyemin Çoşut, Department of Chemistry, Gebze Technical University, P.O.Box: 141, Gebze 41400, Kocaeli, Turkey

Tel: 00 90 262 6053015

Fax: 00 90 262 6053105

e-mail: bc@gtu.edu.tr

Abstract

The synthesized and sensing capability of two novel azaindole substituted mono and distyryl BODIPY dyes against bisulfate anion were reported. Structural characterizations of the targeted compounds were conducted by using matrix-assisted laser desorption/ionization time-of-flight mass spectrometry, ^{1}H and ^{13}C NMR spectroscopies. Photophysical properties of the azaindole substituted BODIPY compounds were investigated employing absorption and fluorescence spectroscopies in acetonitrile solution. It was found that the final compounds **3** and **4** exhibited exclusively selective and sensitive turn-off sensor behavior on HSO_4^- anion. Additionally, the stoichiometry ratio of the targeted compounds to bisulfate anion was measured 0.5 by Job's method. Also, density function theory was performed to the optical response of the sensor for targeted compounds. Furthermore, the cytotoxicity of Azaindole-BODIPYs were examined against living human leukemia K562 cell lines.

***Keywords**:* Borondipyrromethenes, Azaindole, hydrogen sulfate, Anionsensor, Fluorescence, Chemosensor, K562 cell lines, DFT.

1. Introduction

The construction of cation and anion fluorescent chemosensors has a growing interest over the past years since they play a critical role in chemistry fields related with organic, supramolecular and biological process [1-5]. The extensive researches on metal and pH sensors which have been previously investigated showed that they are important in both biological and environmental processes [6,7]. Particularly, among the variety of anion sensors, the detection of bisulfate (HSO_4^-) anions are extremely important. Firstly, they are found in many agricultural fertilizers, industrial raw materials, nuclear fuel waste and toxic effect in pollutant [8]. Secondly, in the point of their biological applications, HSO_4^- anions dissociate at high pH to generate toxic sulphate (SO_4^{-2}) ions. These toxic ions cause irritation of the skin, eyes and respiratory system [9,10]. Despite this importance, only a few examples have been reported in the literature for detection of HSO_4^- anions [11-15].

The design of fluorescent sensors can be arranged by covalently integrated photoactive fragment(s) with a receptor subunit(s). In this sense, the units of the fluorescent sensors play a critical role for detection of anions. On the one part, as a photoactive fragment in fluorescent sensors, Boron dipyrromethane (BODIPY) has been attractive targets within highly fluorescent dyes over the last few decades [16]. They frequently display an excellent photophysical properties such as high fluorescence quantum yield, large extinction coefficient, high chemical, thermal and photophysical stability [17-20]. Thus, they have a wide range of applications include fluorescent biolabelling reagents, light harvesting materials, optical chemosensor and photodynamic therapy reagents [21-25]. And therefore, structures containing BODIPY scaffolds present fluorescent sensor for both anions and cations [26,27]. On the other part, as a receptor subunit, the azaindole nuclei which have nitrogen containing aromatic heterocyclic compounds can be used. They have a great attention because of their valuable physicochemical and pharmacological properties with

potential application in medicinal chemistry [28-31]. Thus, the combinations of BODIPY and azaindole nuclei can be useful for many applications in chemistry.

Covalently combined BODIPY core and azaindole moieties were reported by Mahapatra et al. [32]. In their study, an azaindole motif placed at the *meso* (8) position of BODIPY core was investigated by ^{1}H NMR, steady-state and emission spectroscopies, suggesting a dual channel detection of fluoride (absorption) and AcO- anions (emission) among various anions. In the present work, we are interested in the combination of BODIPY and azaindole motifs which is at only 3-position (mono) and, both 3- and 5- positions (distryl) of BODIPY (Scheme 1, compound **3** and **4**, respectively) core to investigate their photophysical and anion selectivity properties. It is shown here that the difference in azaindole position with respect to BODIPY core affects the π-electron distributions. However, newly developed compounds enable to detect HSO_4^- anion. Also, we report here in vitro cytotoxicity effects against Human leukemia K562 cell line for titled compounds.

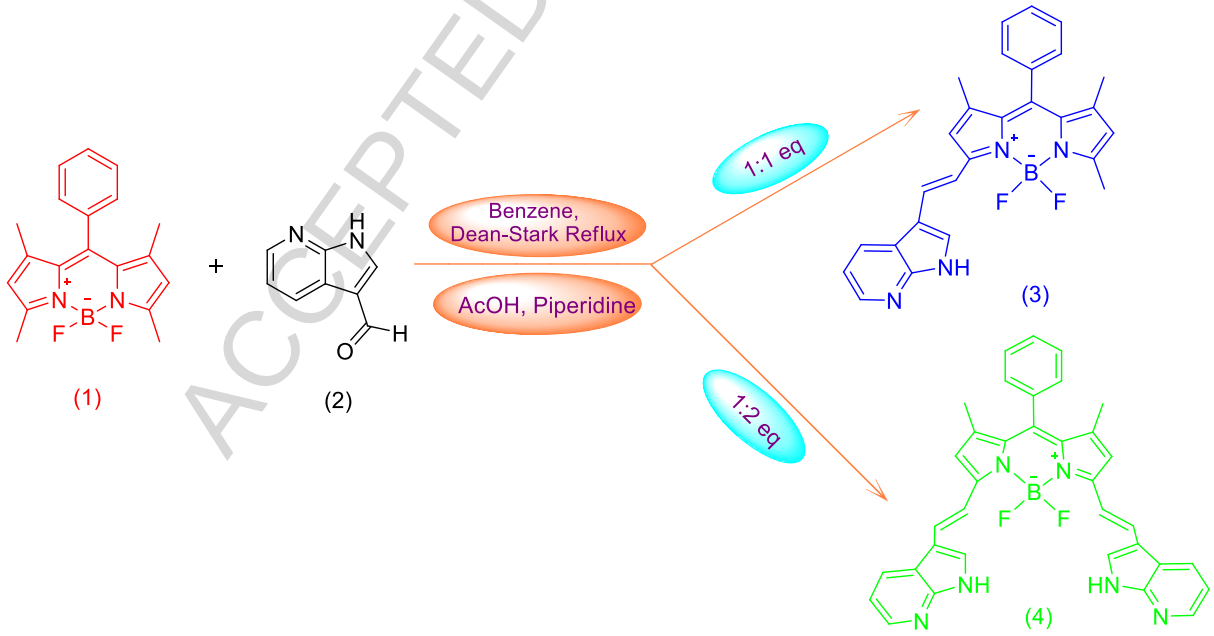

Scheme 1 Chemical structure and synthetic pathway of Azaindole-BODIPYs (**3** and **4**).

2. Experimental

2.1. Materials

The deuterated solvent ($CDCl_3$) for NMR spectroscopy, silica gel, dichloromethane and metal chlorides were provided from Merck. Following chemicals were obtained from Sigma Aldrich; 2,4-dimethylpyrrole, benzaldehyde, trifluoroacetic acid, p-Chloranil, triethylamine, Boron trifluoride diethyl etherate, glacial acetic acid, piperidine, hydrogen peroxide, *N*,*N*-dimethylformamide, benzene and 1,8,9-Anthracenetriol for the MALDI matrix was obtained from Fluka. All other chemicals used for the synthesis were reagent grade unless otherwise specified like sodium anions (I^-, F^-, SO_4^{2-}, HPO_4^{2-}, HSO_4^-, and CH_3COO^-).

2.2. Equipment

Electronic absorption spectra were recorded with a Shimadzu 2101 UV spectrophotometer in the UV-visible region. Fluorescence excitation and emission spectra were recorded on a Varian Eclipse spectrofluorometer using 1 cm pathlength cuvettes at room temperature. The reversibility measurements of the probes were conducted with UV spectrophotometer and Varian Eclipse spectrofluorometer by using 0.1M H_2O_2. The fluorescence lifetimes were obtained using Horiba- Jobin-Yvon-SPEX Fluorolog 3-2iHR instrument with Fluoro Hub-B Single Photon Counting Controller at an excitation wavelength of 470 nm. Signal acquisition was performed using a TCSPC module. Mass spectra were acquired in linear modes with average of 50 shots on a Bruker Daltonics Microflex mass spectrometer (Bremen, Germany) equipped with a nitrogen UV-Laser operating at 337 nm. Elemental analyses were obtained using a Thermo Finnigan Flash 1112 Instrument. ^1H and ^{13}C NMR spectra were recorded in $CDCl_3$ solutions on a Varian 500 MHz spectrometer. Analytical thin layer chromatography (TLC) was performed on silica gel plates (Merck, Kieselgel 60 Å, 0.25 mm thickness) with F_{254} indicator. Column chromatography was

performed on silica gel (Merck, Kieselgel 60 Å, 230-400 mesh). Suction column chromatography was performed on silica gel (Merck, Kieselgel 60 Å, 70-230 mesh).

2.3. The parameters for fluorescence quantum yields

The fluorescence quantum yield value of the compounds **3** and **4** were determined in dichloromethane by comparing with the fluorescence of Rhodamine 6G and ZnPc as a standard, respectively. Fluorescence quantum yields (Φ_F) were calculated by the comparative method (Eq. 1) [33].

$$\Phi_F = \Phi_F(\text{Std}) \frac{F . A_{Std} . n^2}{F_{Std} . A . n^2_{Std}} \quad (1)$$

Where Φ_F(Std) is the fluorescence quantum yield of standard. Rhodamine 6G was employed as the standard for compound **3** (Φ_F = 0.95 in water) [34]. Unsubstituted ZnPc was employed as the standard (Φ_F = 0.18 in DMSO) for compound **4** [35]. F and F_{Std} are the areas under the fluorescence emission curve of sample and the standard, respectively. A and A_{Std} are the respective absorbance of the samples and standard at the excitation wavelengths. η^2 and η^2_{Std} are the refractive indices of solvents used for the sample and standard, respectively. The concentration of the solutions at the excitation wavelength fixed at $2x10^{-6}$ mol.dm^{-3}.

2.4. Computational Methods

The ground state geometries were created by Density Functional Theory (DFT) [36]. After running an optimization, harmonic vibrational frequencies were computed to test performed optimization. It was revealed that there were no negative frequencies. The absence of imaginary frequencies confirmed that the optimization was successfully completed by chosen method and basis set. In addition to ground state optimization, electron densities of the targeted compounds were investigated by HOMO-LUMO frontier orbitals theory. All the computations were performed by Gaussian 09 program [37] on a personal computer using

B3LYP [38] in conjunction with the 6-31G(d,p) and LANL2DZ basis set for anions. Visualization of the structures was examined by GaussView program [39].

2.5. Cell lines and cell culture

In this study, human chronic myeloid leukemia cell line (K562) was used. Cells were cultured in RPMI 1640 medium (Lonza, Switzerland) supplemented with 10% FBS (Biochrom, Germany) and gentamycin (Biological Industries, USA) at 37°C in a humidified atmosphere with 5% CO_2.

2.6. Cytotoxicity assay

Cell viabilities were determined by 3-(4,5-dimethylthiazol-2-yl)-2,5 diphenyltetrazolium bromide (MTT) assay (Serva Electrophoresis GmBH, Germany) as described previously. 1x104 cells/well were seeded into 96-well microplates and incubated for 48 h. Then, cells were washed with phosphate buffered saline (PBS) twice and medium was renewed, and cells were treated with different concentrations of compounds and incubated for 48 h. Only mediums including corresponding amount of the compounds were used as blanks, and acetonitrile, by which compounds were dissolved, treated cells were used as control. Next, cells were washed with PBS twice, medium was renewed and 10 µl/well MTT solutions (5 mg/ml dissolved in PBS) were added onto cells. Cells were incubated at 37 ºC and 5% CO_2 for 4 h and disrupted by 100 µl/well SDS-HCl solution (10% SDS and 0,01 M HCl) overnight. Microplates were read at 570 nm by the microplate spectrophotometer (Multiskan GO; Thermo Fisher Scientific, USA). Optical density values were converted cell viabilities by using acetonitrile-treated cells as references (100%). Inhibitory concentration 50 (IC50) referring to the concentration which inhibits half of the cells was calculated from the logarithmically plotted graph of concentration-cell viabilities for each treatment.

2.7. Statistical analyses

Cytotoxicity assay was repeated three times as independent experiments with each set containing quadrate of the same treatment (n=12). Results were analyzed by GraphPad Prism 6 (GraphPad Software, Inc., USA) with Student's T-Test and significant when $p<0.05$.

2.8. Synthesis

Compound **1** [27] and compound **2** [40] were synthesized and purified according to literature procedure.

2.8.1. Synthesis of compound 3

A solution of compound **1** (100.0 mg, 0.31 mmol) and compound **2** (45.1 mg, 0.31 mmol) in benzene (30 mL) was treated with piperidine (180 µL) and acetic acid (180 µL) respectively. The reaction mixture was heated under reflux using Dean-Stark apparatus until all aldehyde was consumed. The reaction mixture was diluted with water and extracted with dichloromethane. The combined organic layers washed with brine and dried over sodium sulphate. The solvent was evaporated, and the product was purified by column chromatography (SiO_2, 90%-10% dichloromethane/methanol) to give compound **3** (30.0 mg, 22%). Anal. Calc. for $C_{27}H_{23}BF_2N_4$: C, 71.70; H, 5.13; N, 12.39; Found: C, 71.73; H, 5.10; N, 12.35 %. MALDI-TOF m/z Calc. 452.20; found 453.56 $[M+H]^+$ ^{1}H NMR (500 MHz, $CDCl_3$) δ_H 8.60 (d, *J* = 16.80 Hz, 2H), (*trans*-CH); 7.70-7.45 (m, 5H+4H, Ar-CH); 6.10 (s, 2H); 2,53 (s, 3H), (CH_3); 1.97 (s, 6H), (CH_3) ppm.^{13}C NMR (126 MHz, $CDCl_3$) δ_C 167.02, 166.53, 151.69, 151.55, 150.25, 143.84, 137.23, 135.60, 130.58, 128.91, 128.66, 128.49, 128.39, 128.03, 127.94, 127.84, 125.12, 124.90, 124.63, 116.97, 116.57, 109.94, 24.49, 24.33, 18.76 ppm.

2.8.2. Synthesis of compound 4

A solution of compound **1** (100.0 mg, 0.31 mmol) and compound **2** (90.5 mg, 0.62 mmol) in benzene (30 mL) was treated with piperidine (370 µL) and acetic acid (370 µL)

respectively. The reaction mixture was heated under reflux using Dean-Stark apparatus until all aldehyde was consumed. The reaction mixture was diluted with water and extracted with dichloromethane. The combined organic layers washed with brine and dried over sodium sulphate. The solvent was evaporated, and the product was purified by column chromatography (SiO_2, 90%-10% dichloromethane/methanol) to give compound **4** (50 mg, 28%). Anal. Calc. for $C_{35}H_{27}BF_2N_6$: C, 72.42; H, 4.69; N, 14.48; Found: C, 72.47; H, 4.65; N, 14.43 %. MALDI-TOF m/z Calc. 580.12; found 581.1 [M+H]. ^{1}H NMR (500 MHz, $CDCl_3$) δ_H 8.11 (d, *J* = 16.80 Hz, 2H), (*trans*-CH); 7.75 (d, *J* = 16.80 Hz, 2H), (*trans*-CH); 7.68-7.41 (m, 5H+8H, Ar-CH), 6.10 (s, 2H), 1.95 (s, 6H), (CH_3) ppm.^{13}C NMR (126 MHz, $CDCl_3$) δ_C 151.89, 151.37, 151.33, 144.81, 143.89, 143.80, 143.71, 143.30, 137.39, 137.15, 136.27, 135.94, 129.74, 129.36, 128.11, 127.99, 127.82, 124.62, 18.70 ppm.

3. Results and Discussion

3.1. Synthesis and Structural Characterization

Azaindole known as pyridine-fused heterocyclic compound was employed as a linker to synthesize monostyryl and distyryl BODIPYs **3** and **4**, respectively. The synthesis strategy began with the formylation of 7-azaindole using hexamethylenetetramine in acetic acid, which gave the corresponding 7-azaindole-3-carbaldehyde **2** [40]. Knoevenagel reaction method was utilized for the preparation of the novel BODIPY-azaindole compounds **3** and **4**. The synthesis pathways for preparation of the compounds **3** and **4** are illustrated in Scheme 1. Accordingly, benzaldehyde (1.0 equiv.) was first treated with 2,4-dimethylpyrrole (2.2 equiv.) in the presence of TFA in dry DCM, followed by oxidation with p-chloranil at room temperature. The resulting dipyrrin intermediate was then treated with Et_3N and $BF_3.Et_2O$ to yield the green fluorescent BODIPY compound **1** [27]. With BODIPY **1** and 7-azaindole aldehyde **2** in hand, it was of interest to synthesize monostyryl **3** before extending the

Knoevenagel reaction to distyryl. The treatment of the compound **1** with **2** in 1:1 molar ratio in the presence of acetic acid and piperidine gave monostyryl BODIPY **3** in 22% yield.

Having successfully used Knoevenagel reaction to synthesize monostyryl BODIPY **3**, attention therefore turned to the preparation of the related distyryl BODIPY. For this purpose, condensation of compound **1** and **2** in 1:2 molar ratio in a Dean-Stark apparatus using standard conditions produced the compound **4** in 28% yield. All new compounds were isolated by column chromatography. Identification of the compounds **3** and **4** were performed through elemental analysis mass spectrometry, ^{1}H and ^{13}C NMR spectroscopy. The results were consistent with the predicted structures, as shown in the synthesis section. The elemental analysis results and the mass spectral data for the newly synthesized BODIPY-azaindole compounds **3** and **4** were consistent with the assigned formulations. The mass spectrum of compound **3** was obtained by MALDI-TOF MS using 1,8,9-anthracenetriol as the MALDI matrix, and the spectrum revealed the peak groups representing the protonated molecular ions at 453.56 Da and molecular ion rupture fluorine at 434.32 Da Figure 1(a). Similarly, the mass spectrum of compound **4** was showed the protonated molecular ions at 580.308 Da and molecular ion rupture fluorine at 561.15 Da Figure 1(b). The aromatic and aliphatic protons were observed between 8.60-6.10 ppm and 2.53-1.95 ppm, respectively in the ^{1}H NMR spectra. The aromatic carbons for compound **4** and **5** were observed between 167.02-109.94 ppm and aliphatic carbons 24.49-18.76 ppm in the ^{13}C NMR spectra.

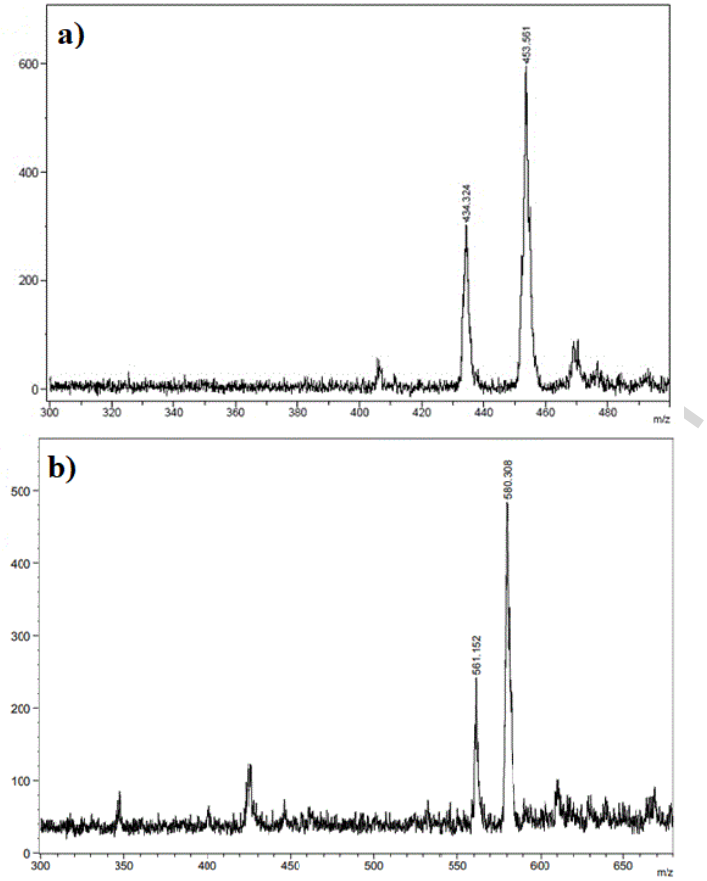

Figure 1 Positive ion and linear mode MALDI TOF-MS spectra of compound **3** (a) and **4** (b).

3.2. Spectral and Chemosensor Studies

Absorption and fluorescence spectra of azaindole-BODIPY compounds in acetonitrile displayed in

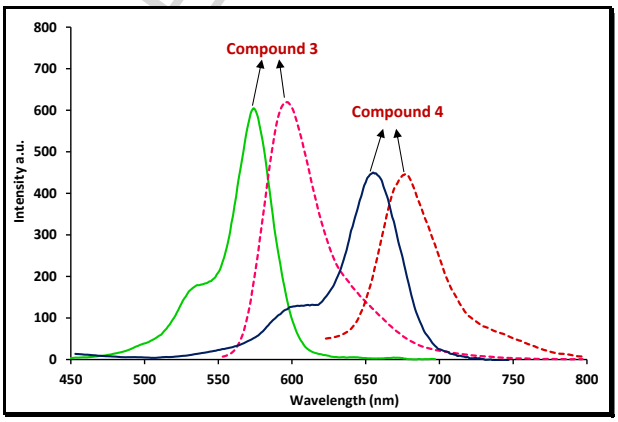

Figure 2 exhibit the red-shift with increasing the electron density of the compounds. While the maximum absorbance wavelength of compounds **3** and **4** were determined at 574

and 655 nm in acetonitrile, the fluorescence emission maxima were found to 595 and 677 nm in the same solution, respectively (

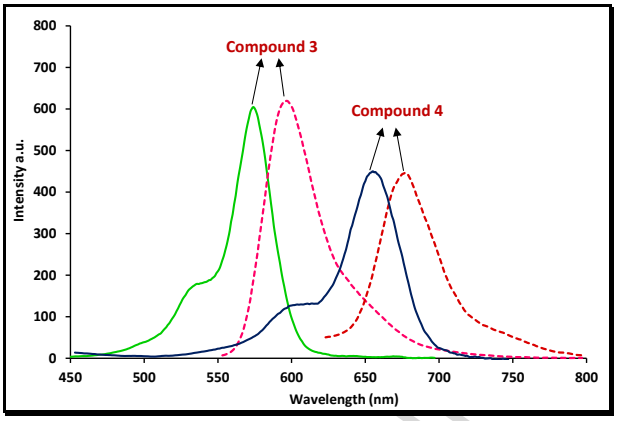

Figure 2). The spectral data of azaindole BODIPY compounds **3** and **4** in acetonitrile were given Table 1. Although it is not the primary issue in this study, the absorption and fluorescence properties of azaindole substituted BODIPYs **3** and **4** were performed in a variety of solvent include methanol, ethanol, toluene, acetonitrile, acetone, dichloromethane, chloroform, dimethylsulfoxide, tetrahydrofuran and benzene at room temperature (Figure S1-S4). Solvent effect on the absorption spectra was revealed that while the lowest absorption wavelength was observed in dichloromethane, the highest absorption wavelength was observed in dimethylsulfoxide for both compounds (Figure S1 and S3). Given the fluorescent emission spectra, despite the decrease fluorescence emission intensity of the compounds in the dimethylsulfoxide solvent, red shift was observed in the fluorescence wavelength.

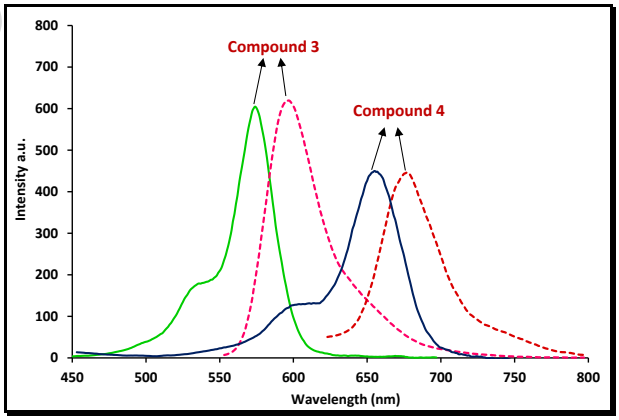

Figure 2 Excitation (solid lines) and emission spectra (dashed lines) of compound **3** and **4** in acetonitrile.

Table 1 Photophysical properties of azaindole- BODIPYs [a]

Compound	λ_{ab}, (nm)	λ_{em}, (nm)	ϵ^b, (10^4 M^{-1} cm^{-1})	Δ_{Stokes}, (nm)	K_a ($10^5 M^{-1}$)	τ_F [c] (ns)	Φ_F [d]	Detection limit, (μM)
3	574	595	2.49	21	1.87	4.173 CHISQ = 1.285	0.42	75.6
4	655	677	1.28	22	6.13	3.763 CHISQ = 1.752	0.14	44.27

[a]Acetonitrile. [b]Molar extinction coefficients. [c]Lifetime . [d] Fluorescence quantum yield.

The fluorescence lifetime spectra are depicted in Figure 3 for the compound **3** and **4**. The data are collected by using the time correlated single photon counting (TCSPC) technique in acetonitrile. The lifetimes were found to be 4.17 and 3.76 ns for compounds **3** and **4,** respectively. Furthermore, the fluorescence quantum yields (Φ_F) of compounds were calculated 0.42 for compound **3** and 0.14 for compound **4**. The fluorescence quantum yield of compound **3** is higher than that of **4** and this situation is compatible with fluorescence lifetime results.

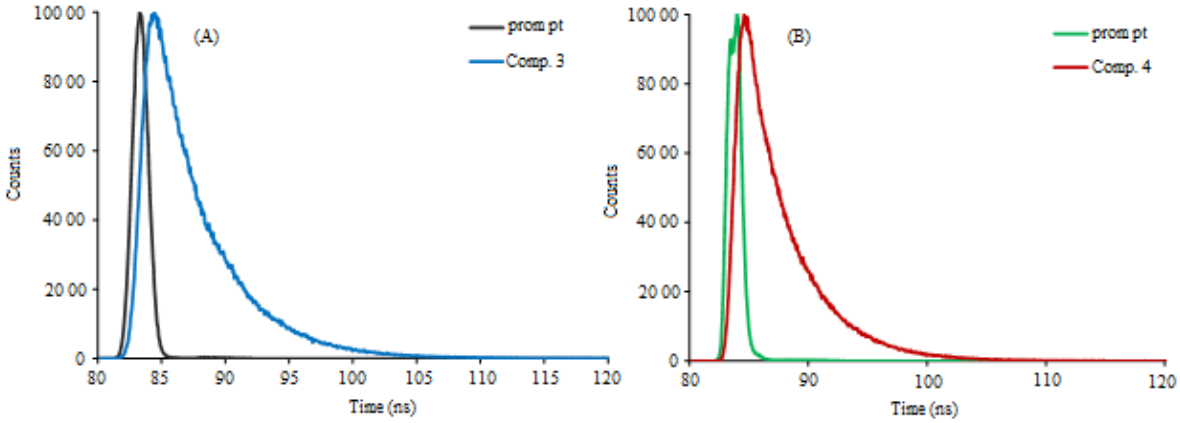

Figure 3 Fluorescence decay profile of azaindole-Bodipys (**3** and **4**) in the presence using laser excitation source of 390 nm.

The chemosensor properties of the synthesized azaindole-BODIPY **3** and **4** against some anions aqueous solutions such as I^-, F^-, SO_4^{2-}, HPO_4^{2-}, HSO_4^-, CH_3COO^- were investigated by UV–Vis and fluorescence spectroscopy. All spectral measurements were performed in acetonitrile solutions. The aqueous solutions of the corresponding sodium anions were used as the source of anions. To investigate the effect of anions on the absorption

and fluorescence properties of the compounds, the working concentrations of the compound **3** and **4** were prepared as 3 μM and 10 μM, respectively. 10 μL of 0.1 M different anions (I^-, F^-, SO_4^{2-}, HPO_4^{2-}, HSO_4^-, CH_3COO^-) was added to the solution to examine the anion effect on the absorption and fluorescence properties of the compounds **3** and **4**. It was revealed that no change in absorption and fluorescence spectra of the titled compounds. Significant changes in the spectra were observed when bisulfate anion (HSO_4^-) was added to compounds. Direct comparison of absorption and emission spectra of the compounds are given at Figure 4. Both compounds exhibit a blue shift (~15 nm) in the absorption spectra (Figure 4(A) and (C)) with addition of HSO_4^- anion comparison with other anions. Furthermore, significant decrease was observed for fluorescence intensities of both compounds (Figure 4(B) and (D)). It was clearly observed that targeted compounds can be found as sensitive "turn-off" fluorescent chemosensor probes for HSO_4^- anions. In addition to these results, direct comparison of our results with a recent report by Mahapatra et al. suggest that the position of azaindole moieties respect to BODIPY core play a significant role for chemosensor properties [32, 41]. It is worth mentioning while BODIPY with an azaindole group at 8 position is sensitive to CH_3COO^-, in 3 and 5 position of BODIPY do not give any respond to CH_3COO^- anion (Figure 4). Our results are consistent with importance of positional effect presents in literature.

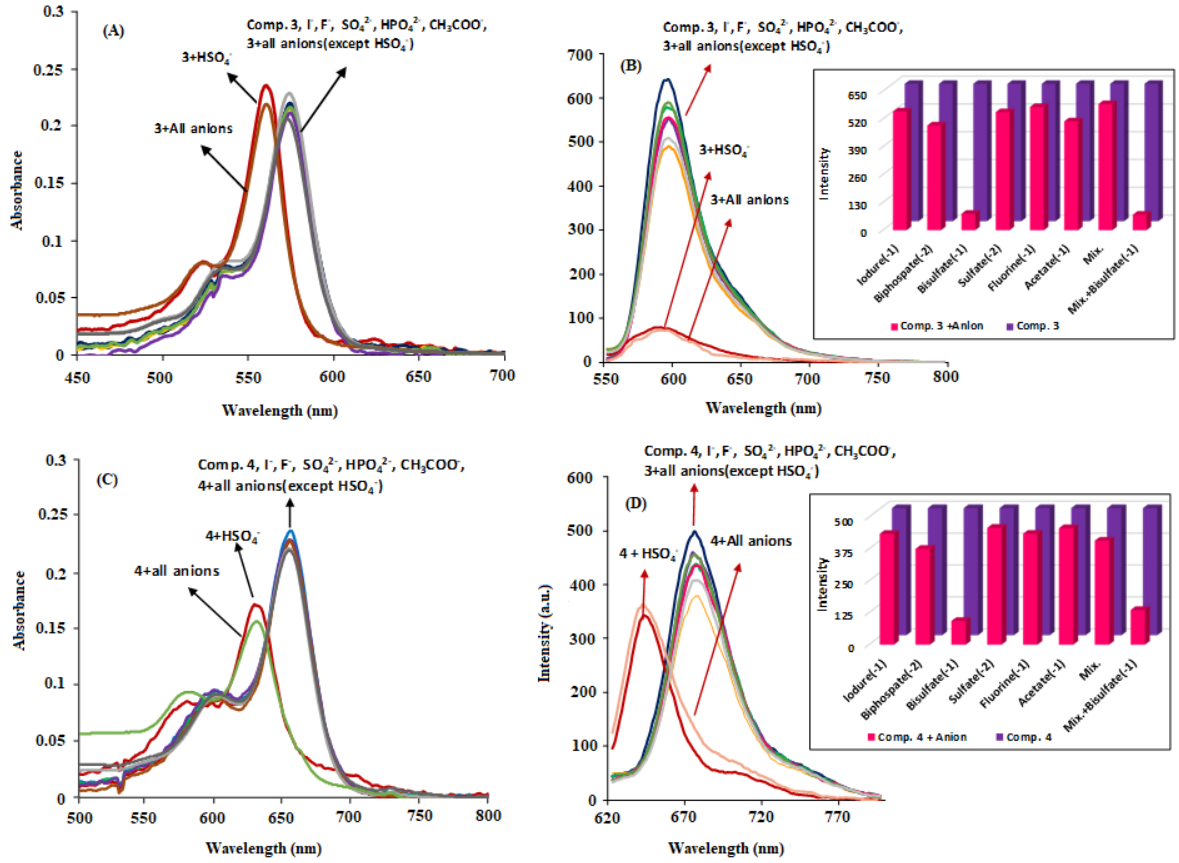

Figure 4 Absorption and emission spectra of compound 3 (A and B) and 4 (C and D) in 3 μM in acetonitrile. The data are recorded after addition of 10 μL of 0.1 M different anion solution. The inserted bar graphs show metal ions selectivity of compounds 3 (upper) and 4 (below). The purple bars represent the fluorescent intensity of the compounds and the red bars indicate the fluorescent intensity of the compounds with various ions.

The Continuous Variation method was employed for the determination of the stoichiometry between the compound **3** and **4** and HSO_4^- anion. According to Job's plot analysis results, the maximum mole fractions for HSO_4^- anion were observed as 0.5 for both compounds. Namely, azaindole-BODIPY compound **3** and **4** and HSO_4^- anions preferred 1:1(L/M) stoichiometry for the formation of complexes between the fluorescent probe and anion in solution (Figure 5(A) and (C)). As shown in Figure 5(B) and (D), fluorescence titration experiments with bisulfate anion were performed to obtain more information on the change in fluorescence properties of azaindole-BODIPY compounds **3** and **4** in the presence of bisulfate anion (0-125x10^{-5} M for compound **3** and 0-65x10^{-5} M for comp. **4**). Additionally, the detection limit (DL) and association constant (Ka) were determined based on the

fluorescence titration data [42] (Figure 6). According to the fluorescence titration curve, limits of detection of bisulfate anion for sensors were calculated as 75.6 and 44.27 μM for compounds **3** and **4**, respectively (Table 1). The association constant (Ka) of azaindole-BODIPY compounds with HSO_4^- anion were determined using the Benesi–Hildebrand equation as follows:

$$\frac{1}{I_0 - I} = \frac{1}{K_a x (I_{max} - I_0) x [HSO_4^-]} + \frac{1}{I_{max} - I_0}$$

According to this equation, Ka values for compounds (**3** and **4**) were calculated as 1.87×10^5 M^{-1} and 6.13×10^5 M^{-1}, respectively. The Ka value of compound **4** is higher than that of compound **3**, and consistent with this result, compound **4** has a lower detection limit than **3**.In addition to these photophysical studies, reversibility of the samples was also investigated. The Compound 3-HSO_4^- and Compound 4-HSO_4^- solution were treated with 40 μL 0.1 M H_2O_2 (Figure S7) [43] This result indicating that the coordination of the sensor with HSO_4^- is chemically reversible.

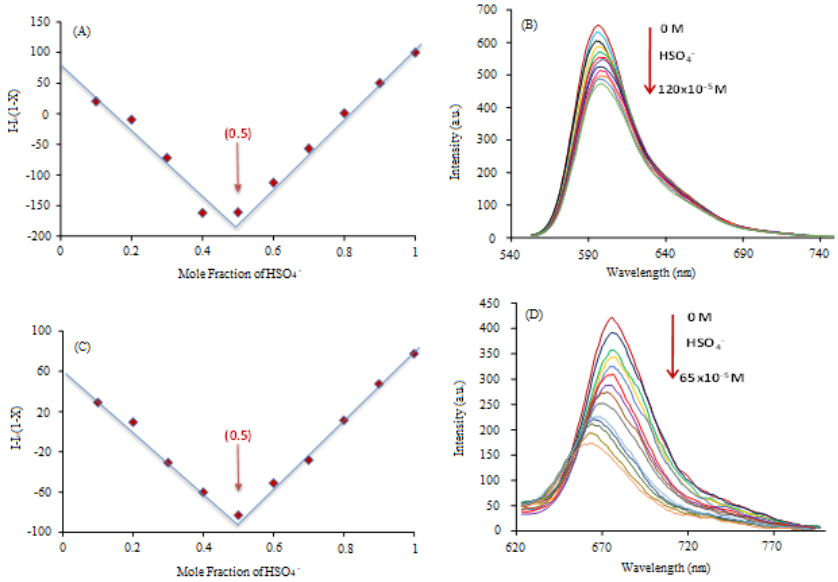

Figure 5 Job's plots of fluorescence of compound 3 (A) and 4 (C) mixed with HSO_4^- anion. Fluorescence titration of compound 3 (B) and (D) with different amount of HSO_4^- anion. All data recorded in 3 μM in acetonitrile. Excitation wavelength is nm.

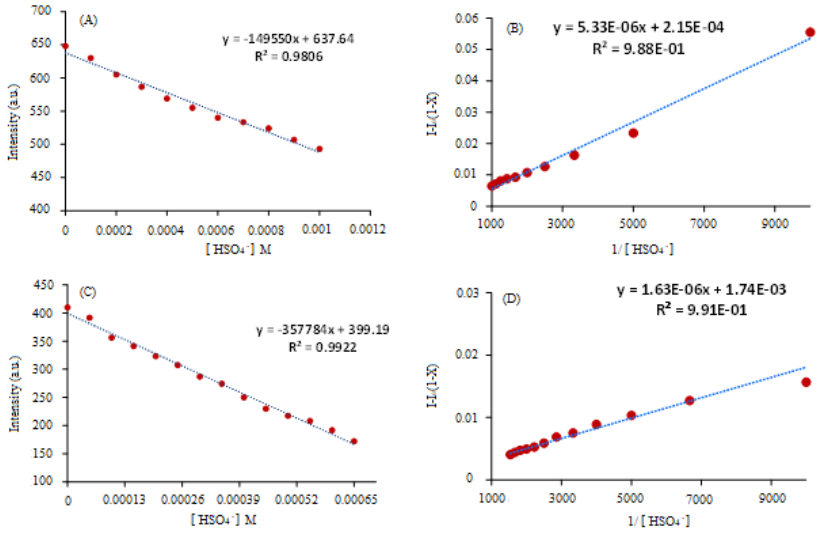

Figure 6 Calibration curve of fluorescence intensity for compound 3 (A) and 4 (C). Benesi–Hildebrand Plot of $1/I_0$-I against 1/[HSO_4-] for compound 3 (B) and 4 (D). All data recorded in acetonitrile.

3.3. Computational results

The results given in previous section comparison with recent report [32] show a clear positional effect for azaindole moieties respect to BODIPY core on chemosensor properties for azaindole-BODIPY compounds. To find out the origin of this effect, we carried out quantum mechanical calculations to determine the relaxed geometries and their HOMO-

LUMO orbitals energies. The all calculations were carried out by means of B3LYP function with 6-31G(d,p) for both compounds. Firstly, we will focus on optimized geometries for the compound **3**, **4** and modelled structures. Their optimized geometries are given in Figure 7(A). The dihedral angles between the methyl groups in the BODIPY dye and hydrogens in the benzene ring are ~ 90° due to the repulsion interaction. After optimization, Electro Static Potential (ESP) map was created for compound **3** and **4**. The ESP maps are given at Figure 8. The most positive charge is located at around the NH in azaindole indole units. Thus, the HSO_4^- anions are interacted with these parts of the compounds (Figure 7(B)) since experimental data indicate that maximum mole fractions for HSO_4^- anion is 0.5 for both compounds (Figure 5). The optimizations are completed for three different modelled structures labeled as model 1, model 2 and model 3 (Figure 7B). Model 1 is for compound **3** interacted with HSO_4^- anion. Model 2 and model 3 are for compound **4**. Model 2 and 3 differ only the position of anion with azaindole moieties. Model 2 is interacted only one azaindole moieties and the other model is with both moieties. The calculations are carried out by the same level of theory with additionally LANL2DZ basis set for anions. The results showed that the geometric parameters of the modelled structures are slightly changed comparison with titled compounds (Figure 7(A) and Figure 7(B)) and model 3 is most stable than model 2 (Figure 7B). Thus, model 3 expected to likely lead to experimental data observed here for compound 4 with HSO_4^- anion.

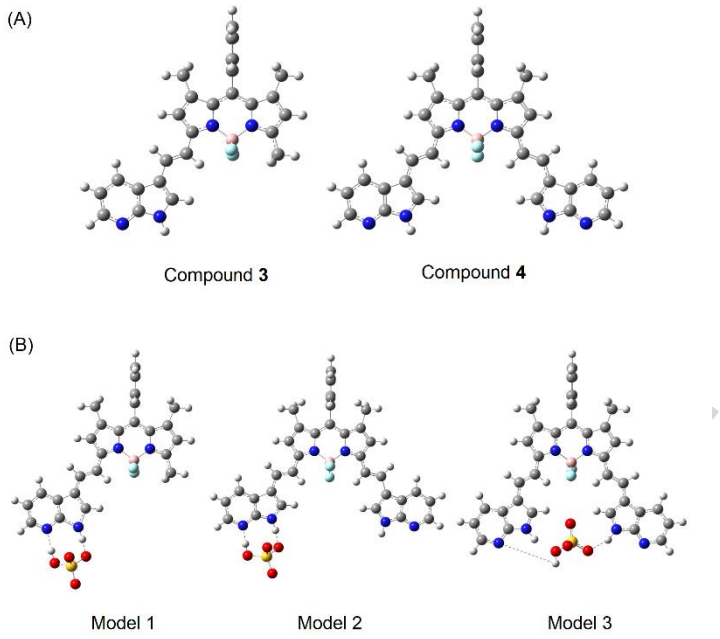

Figure 7 The optimized structures of (A) compound **3** and compound **4**, (B) compound **3** and **4** modelled with HSO_4^- anion.

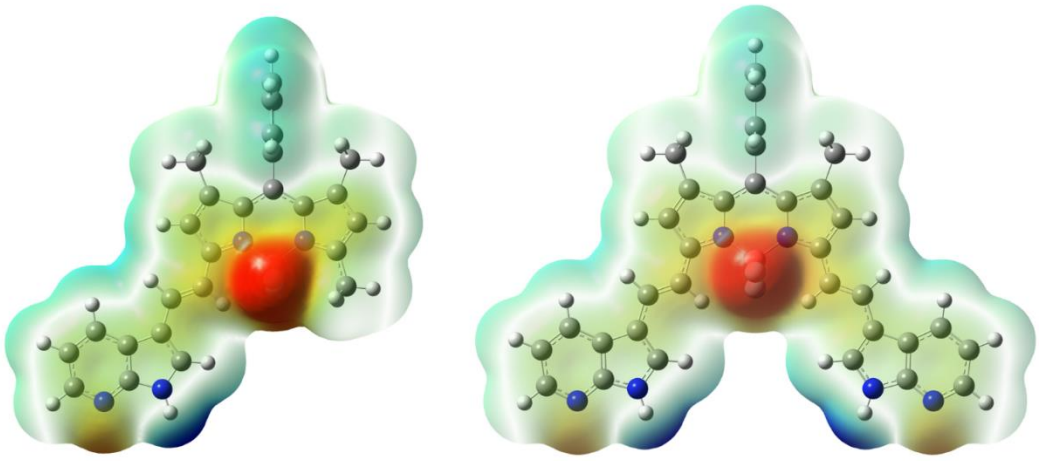

Figure 8 The ESP colored maps for compound 3 (left) and compound 4 (right).

Secondly, having the optimized geometries for compounds and modelled structures given at Figure 7(A) and (B), our attention turned to analyze the HOMO and LUMO orbitals to complement experimental observations. The orbitals were created by the same level of theory. The frontier orbitals for compound **3** and **4** are given at Figure 9. The HOMO orbital

energies are -4.85 and -4.59 eV for compound **3** and **4**, and the LUMOs are -2.38 and -2.44 eV for the same order. Their calculated energy gabs are -2.47 eV and -2.15 eV for compound **3** and **4**, respectively. The results indicated that compound **4** has smaller gab than compound **3**. Accordingly, this predicted energy gabs can be explain the result of fluorescence life time measurements which is compound **4** has shorter fluorescence lifetime than compound **3**. Here, also, it is important to take attention that the position of azaindole moiety affects to electron distributions. Direct comparison of an azaindole motif placed at the *meso* (8) position [32] and 3-position (mono) of BODIPY (compound **3**, in this study) showed that HOMO and LUMO orbitals are located at only BODIPY core for meso position of azaindole moiety and electrons are more distributed for compound **3** (Figure 9) decreasing with the band gab. This comparison indicates that perpendicular position of azaindole moiety respect to BODIPY core causes blocking of electron conjugation. This observation might be the reason for different selectivity properties of BODIPY core with azaindole moiety for detection of different anions. Moreover, the HOMO orbital energies for model 1**,** model 2 and model 3 are -5.94, -6.10 and -5.83 eV, respectively. The LUMO orbital energies are -3.63, -3.15 and -3.09 eV, with the same order.

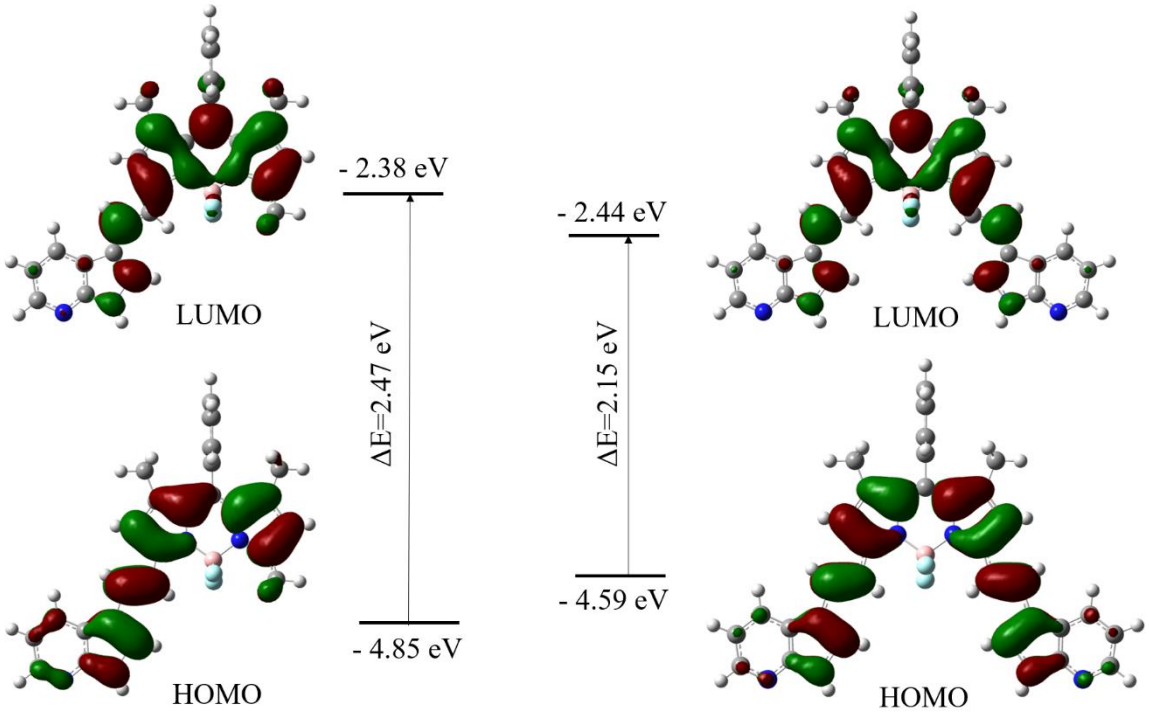

Figure 9 The frontier orbitals for compound 3 (left) and compound 4 (right).

3.4. Biological properties

The novel azaindole-BODIPYs **3** and **4** were tested for their cytotoxicity activity since azaindole derivates have been widely shown to inhibit important kinases [44-46]. The cytotoxicity of the azaindole-BODIPY conjugates was assessed against K562 cell lines. The cells were treated with increasing concentrations of compounds **3** and **4**. Also, the cells were treated with these concentrations of compounds **3** and **4** in the presence of 1 μM of $NaHSO_4$ to determine whether the treatment of $NaHSO_4$ was influencing cytotoxicities. The biological studies revealed that both compound **3** and **4** were able to inhibit cell viabilities efficiently (Figure 10). The novel monostyryl and distyryl BODIPYs displayed cytotoxic activity alone with IC_{50} values of 0,621 ± 0,04 and 0,764 ± 0,079 against K562 cell lines, respectively (Table 2). Moreover, the presence of $NaHSO_4$ in the targeted BODIPY scaffolds, **3** and **4** could not significantly alter the IC_{50} values; 0,835 ± 0,246 for compound **3** plus $NaHSO_4$ and 0,752 ± 0,076 for compound **4** plus $NaHSO_4$ ($p<0.05$). Preliminary biological assays indicate

that BODIPY platforms containing azaindole moiety have a moderate impact on the viability and proliferation of the K562 cell lines cancer cell line.

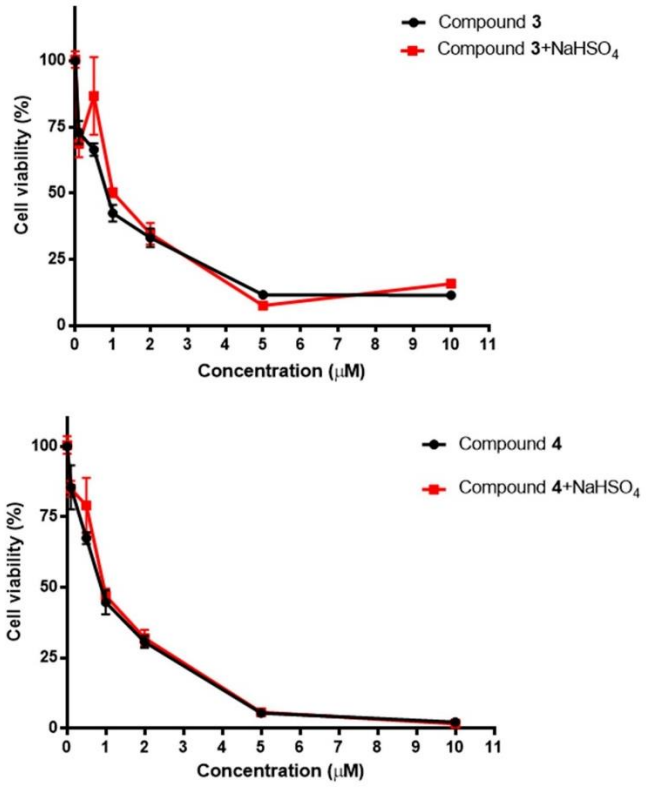

Figure 10 Concentration-cell viability correlations of compound 3, compound 3 plus $NaHSO_4$, compound 4 and compound 4 plus NaHSO4.

Table 2 IC_{50} values for related treatments.

Compounds	**IC50 (μM)**
Compound 3	0,621 ± 0,04
Compound 3+$NaHSO_4$	0,835 ± 0,246
Compound 4	0,764 ± 0,079
Compound 4+$NaHSO_4$	0,752 ± 0,076

4. Conclusion

Two new fluorescent chemosensor candidates for bisulphate anion were successfully constructed from azaindole and BODIPY platforms. Structures of obtained monostryl and distryl BODIPYs were clarified and photophysical studies were investigated. According to spectral results, observations on blue shift in absorbance spectra and meaning decreases in fluorescent intensities of both compounds indicated that these two hybrids BODIPYs **3** and **4** can sense bisulphate anion. Conducted computational studies showed that compound **3** has higher gap than compound **4**. We conclude that the final Azaindole-BODIPYs can be used as fluorescent bisulphate anion sensor. A direct comparison of the positionally different placed of azaindole moiety respect to BODIPY core plays a critical role for selectivity and sensitivity for anions. Preliminary biological test indicates that the synthesized azaindole substituted BODIPYs can be valuable candidate as chemotherapeutic agents in cytotoxicity applications. It is expected that the development of these probes will gain great attention in chemistry, biology, and medicine science due to the significant harmful effect of bisulphate anion on human health.

References

[1] P.A. Gale, S.E. García-Garrido, J. Garric, Anion receptors based on organic frameworks: Highlights from 2005 and 2006, Chem. Soc. Rev. 37 (2008) 151–190.

[2] R. Martínez-Máñez, F. Sancenón, Chemodosimeters and 3D inorganic functionalised hosts for the fluoro-chromogenic sensing of anions, Coord. Chem. Rev. 250 (2006) 3081–3093.

[3] C. Suksai, T. Tuntulani, Chromogenic anion sensors, Top. Curr. Chem. 255 (2005) 163–198.

[4] C. Caltagirone, P.A. Gale, T. Review, C. Caltagirone, P.A. Gale, Anion receptor chemistry : highlights from 2007, Coord. Chem. Rev. 38 (2009) 79–128.

[5] B. Valeur, Design principles of fluorescent molecular sensors for cation recognition, Coord. Chem. Rev. 205 (2000) 3–40.

[6] H.L. Corwin, R.A. Bray, M.H. Haber, The detection and interpretation of urinary eosinophils, Arch. Pathol. Lab. Med. 113 (1989) 1256–1258.

[7] S. Mizukami, T. Nagano, Y. Urano, A. Odani, K. Kikuchi, A fluorescent anion sensor that works in neutral aqueous solution for bioanalytical application, J. Am. Chem. Soc. 124 (2002) 3920–3925.

[8] B.A. Moyer, F. V. Sloop, C.J. Fowler, T.J. Haverlock, H.A. Kang, L.H. Delmau, D.M. Bau, M.A. Hossain, K. Bowman-James, J.A. Shriver, N.L. Bill, D.E. Gross, M. Marquez, V.M. Lynch, J.L. Sessler, Enhanced liquid-liquid anion exchange using macrocyclic anion receptors: Effect of receptor structure on sulphate-nitrate exchange selectivity, Supramol. Chem. 22 (2010) 653–671.

[9] D.G. Cho, H.K. Jong, J.L. Sessler, The benzil-cyanide reaction and its application to the development of a selective cyanide anion indicator, J. Am. Chem. Soc. 130 (2008) 12163–12167.

[10] P.S. Shah, T. Balkhair, Air pollution and birth outcomes: A systematic review, Environ. Int. 37 (2011) 498–516.

[11] S.T. Yang, D.J. Liao, S.J. Chen, C.H. Hu, A.T. Wu, A fluorescence enhancement-based sensor for hydrogen sulfate ion, Analyst. 137 (2012) 1553–1555.

[12] W. Xue, L. Li, Q. Li, A. Wu, Novel furo[2,3-d] pyrimidine derivative as fluorescent chemosensor for HSO^{4-}, Talanta. 88 (2012) 734–738.

[13] P. Li, Y.M. Zhang, Q. Lin, J.Q. Li, T.B. Wei, A novel colorimetric HSO 4- sensor in aqueous media, Spectrochim. Acta - Part A Mol. Biomol. Spectrosc. 90 (2012) 152–157.

[14] H.J. Kim, S. Bhuniya, R.K. Mahajan, R. Puri, H. Liu, K.C. Ko, J.Y. Lee, J.S. Kim, Fluorescence turn-on sensors for HSO4-, Chem. Commun. (2009) 7128–7130.

[15] R. Shen, X. Pan, H. Wang, L. Yao, J. Wu, N.T.-D. Transactions, U. 2008, Selective colorimetric and fluorescent detection of HSO^{4-} with sodium (i), magnesium (ii) and

aluminium (iii) xanthone-crown ether complexes, Pubs.Rsc.Org. (n.d.). http://pubs.rsc.org/en/content/articlehtml/2008/dt/b719407b (accessed July 4, 2018).

[16] Y. Ni, J. Wu, Far-red and near infrared BODIPY dyes: Synthesis and applications for fluorescent pH probes and bio-imaging, Org. Biomol. Chem. 12 (2014) 3774–3791.

[17] G. Ulrich, R. Ziessel, A. Harriman, The chemistry of fluorescent bodipy dyes: Versatility unsurpassed, Angew. Chemie - Int. Ed. 47 (2008) 1184–1201.

[18] J.Y. Liu, H.S. Yeung, W. Xu, X. Li, D.K.P. Ng, Highly efficient energy transfer in subphthalocyanine - BODIPY conjugates, Org. Lett. 10 (2008) 5421–5424.

[19] K.M. Kadish, K.M. Smith, R. Guilard, Handbook of Porphyrin Science: With Applications to Chemistry, Physics, Materials Science, Engineering, Biology and Medicine, Volumes 16-20, World Scientific, 2011.

[20] I.F. Sengul, E. Okutan, H. Kandemir, E. Astarci, B. Çoşut, Carbazole substituted BODIPY dyes: Synthesis, photophysical properties and antitumor activity, Dye. Pigment. 123 (2015) 32–38.

[21] T. Cheng, Y. Xu, S. Zhang, W. Zhu, X. Qian, L. Duan, A highly sensitive and selective OFF-ON fluorescent sensor for cadmium in aqueous solution and living cell, J. Am. Chem. Soc. 130 (2008) 16160–16161.

[22] M.C. Yee, S.C. Fas, M.M. Stohlmeyer, T.J. Wandless, K.A. Cimprich, A cell-permeable, activity-based probe for protein and lipid kinases, J. Biol. Chem. 280 (2005) 29053–29059.

[23] M.D. Yilmaz, O.A. Bozdemir, E.U. Akkaya, Light harvesting and efficient energy transfer in a boron-dipyrrin (BODIPY) functionalized perylenediimide derivative, Org. Lett. 8 (2006) 2871–2873.

[24] A. Gorman, J. Killoran, C. O'Shea, T. Kenna, W.M. Gallagher, D.F. O'Shea, In vitro demonstration of the heavy-atom effect for photodynamic therapy, J. Am. Chem. Soc. 126 (2004) 10619–10631.

[25] E.T. Eçik, E. Özcan, H. Kandemir, I.F. Sengul, B. Çoşut, Light harvesting systems composed of carbazole based subphthalocyanine-BODIPY enhanced with intramolecular fluorescence resonance energy transfer (FRET), Dye. Pigment. 136 (2017) 441–449.

[26] Y. Shiraishi, H. Maehara, T. Sugii, D. Wang, T. Hirai, A BODIPY – Indole Conjugate as a Colorimetric and Fluorometric Probe for Fluoride Anion Detection, Tetrahedron Lett. 50 (2008) 1–7.

[27] S.O. Tümay, E. Okutan, I.F. Sengul, E. Özcan, H. Kandemir, T. Doruk, M. Çetin, B. Çoşut, Naked-eye fluorescent sensor for Cu(II) based on indole conjugate BODIPY dye, Polyhedron. 117 (2016) 161–171.

[28] S.M. Twine, L. Murphy, R.S. Phillips, P. Callis, M.T. Cash, A.G. Szabo, The photophysical properties of 6-azaindole, J. Phys. Chem. B. 107 (2003) 637–645.

[29] S. Bin Zhao, S. Wang, Luminescence and reactivity of 7-azaindole derivatives and complexes, Chem. Soc. Rev. 39 (2010) 3142–3156.

[30] J.Y. Mérour, F. Buron, K. Plé, P. Bonnet, S. Routier, The azaindole framework in the design of kinase inhibitors, Molecules. 19 (2014) 19935–19979.

[31] A.A. Prokopov, L.N. Yakhontov, Methods of synthesis and the production technology of therapeutic substance, Pharm. Chem. J. 28 (1994) 471–506.

[32] A.K. Mahapatra, R. Maji, K. Maiti, S.S. Adhikari, C. Das Mukhopadhyay, D. Mandal, Ratiometric sensing of fluoride and acetate anions based on a BODIPY-azaindole platform and its application to living cell imaging, Analyst. 139 (2014) 309–317.

[33] S. Fery-Forgues, D. Lavabre, Are Fluorescence Quantum Yields So Tricky to Measure? A Demonstration Using Familiar Stationery Products, J. Chem. Educ. 76 (1999) 1260-1265.

[34] D. Magde, G.E. Rojas, P.G. Seybold, Solvent dependence of the fluorescence lifetimes of xanthene dyes, Photochem. Photobiol. 70 (1999) 737–744.

[35] P. Jacques, A.M. Braun, Laser Flash Photolysis of Phthalocyanines in Solution and Microemulsion, Helv. Chim. Acta. 64 (1981) 1800–1806.

[36] W. Kohn, L.J. Sham, Self-consistent equations including exchange and correlation effects, Phys. Rev. 140 (1965).

[37] G.E.S. M. J. Frisch, G. W. Trucks, H. B. Schlegel, B.M. M. A. Robb, J. R. Cheeseman, G. Scalmani, V. Barone, H.P.H. G. A. Petersson, H. Nakatsuji, M. Caricato, X. Li, M.H. A. F. Izmaylov, J. Bloino, G. Zheng, J. L. Sonnenberg, T.N. M. Ehara, K. Toyota, R. Fukuda, J. Hasegawa, M. Ishida, J. Y. Honda, O. Kitao, H. Nakai, T. Vreven, J. A. Montgomery, E.B. J. E. Peralta, F. Ogliaro, M. Bearpark, J. J. Heyd, J.N. K. N. Kudin, V. N. Staroverov, T. Keith, R. Kobayashi, J.T. K. Raghavachari, A. Rendell, J. C. Burant, S. S. Iyengar, J.B.C. M. Cossi, N. Rega, J. M. Millam, M. Klene, J. E. Knox, R.E.S. V. Bakken, C. Adamo, J. Jaramillo, R. Gomperts, J.W.O. O. Yazyev, A. J. Austin, R. Cammi, C. Pomelli, G.A.V. R. L. Martin, K. Morokuma, V. G. Zakrzewski, A.D.D. P. Salvador, J. J. Dannenberg, S. Dapprich, J.C. O. Farkas, J. B. Foresman, J. V. Ortiz, D.J. Fox, Gaussian 09, Revision D.01, (2013).

[38] A.D. Becke, Density-functional thermochemistry. III. The role of exact exchange, J. Chem. Phys. 98 (1993) 5648.

[39] R. D. Dennington, T.A. Keith, J.M. Millam, GausView 5.0.8, (2008).

[40] R. Bahekar, M. Jain, P. Jadav, V. Prajapa, D. Patel, A. Gupta, A. Sharma, R. Tom, D. Bandyopadhya, H. Modi, P. Patel, Synthesis and antidiabetic activity of 2, 5-disubstituted-3-imidazol-2-yl-pyrrolo pyridines, Bioorg Med Chem. 15 (2007) 6782-6795.

[41] X.X. He, J. Zhang, X.G. Liu, L. Dong, D. Li, H.Y. Qiu, S.C. Yin, A novel BODIPY-based colorimetric and fluorometric dual-modal chemosensor for Hg^{2+} and Cu^{2+}, Sensors and Actuators B: Chemical 192 (2014) 29-35.

[42] C.A. Parker, W.T. Rees, Correction of fluorecence spectra and measurment of fluorescence quantum efficiency, Pubs.Rsc.Org. 85 (1960) 587–600. http://pubs.rsc.org/en/content/articlepdf/1960/an/an9608500587 (accessed July 4, 2018).

[43] W. Zhang, T. Liu, F. Huo, P. Ning, X. Meng, C.Yin, Reversible Ratiometric Fluorescent Probe for Sensing Bisulphate/H_2O_2 and Its Application in Zebrafish, Anal. Chem. 15 (2017) 8079-8083.

[44] A. Trejo, H. Arzeno, M. Browner, S. Chanda, S. Cheng, D.D. Comer, S.A. Dalrymple, P. Dunten, J.A. Lafargue, B. Lovejoy, J. Freire-Moar, J. Lim, J. McIntosh, J. Miller, E. Papp, D. Reuter, R. Roberts, F. Sanpablo, J. Saunders, K. Song, A. Villasenor, S.D. Warren, M. Welch, P. Weller, P.E. Whiteley, L. Zeng, D.M. Goldstein, Design and Synthesis of 4-Azaindoles as Inhibitors of p38 MAP Kinase, J. Med. Chem. 46 (2003) 4702–4713.

[45] J. Porter, S. Lumb, R.Franklin, J. G-Simorte, M. Calmiano, K. Riche, B. Lallemand, J. Kayaerts, H. Edwards, A. Maloney, J. Delgado, L. King, A. Foley, F. Lecomte, J, Reuberson, C. Meier, M. Batchelor, Bioorg Med Chem. Discovery of 4-azaindoles as novel inhibitors of c-Met kinase, 19 (2009) 2780-2784.

[46] G.F. Lasker, E.A. Pankey, A. V. Allain, S.N. Murthy, J.P. Stasch, P.J. Kadowitz, The selective Rho-kinase inhibitor azaindole-1 has long-lasting erectile activity in the rat, Urology. 81 (2013) 465.e7-465.e14.

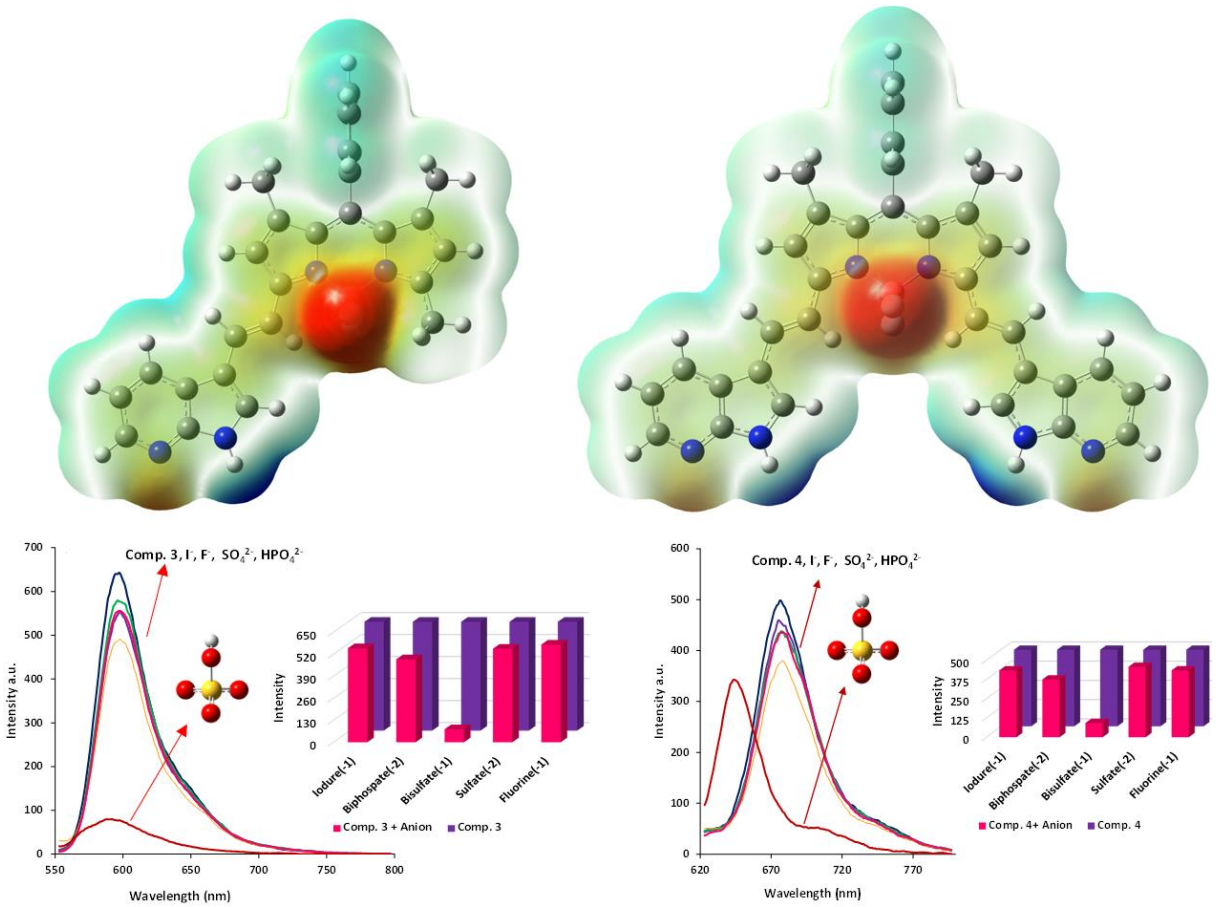

Graphical abstract

Highlights

► New azaindole substituted mono and distyryl BODIPYs have been synthesized.► The Fluorescence Sensing properties of the compounds have been studied in acetonitrile► The cytotoxicity of Azaindole-BODIPYs were examined against living human leukemia K562 cell lines.► Very selective and sensitive fluorescence sensor for detection of HSO4- anion has been obtained.